# Decoupled Kalman Filters for Phased Array Radar Tracking

FREDERICK E. DAUM AND ROBERT J. FITZGERALD

*Abstract*—Kalman filters have been used in numerous phased array radars to track satellites, reentry vehicles, and missiles. This paper considers the design of these filters to reduce computational requirements, ill-conditioning, and the effects of nonlinearities. Several special coordinate systems used to represent the Kalman filter error covariance matrix are described. These covariance coordinates facilitate the approximate decoupling required for practical filter design. A tutorial discussion and analysis of ill-conditioning in Kalman filters is used to motivate these design considerations. This analysis also explains several well-known phenomena reported in the literature. In addition, a discussion of nonlinearities and methods to mitigate their ill effects is included.

## I. Introduction

KALMAN filters have been applied in many phased array radars to track satellites, missiles, reentry vehicles, and other objects. Table I summarizes the major characteristics of both the radar and the particular Kalman filter in these applications. All of these radars have rather large antennas (up to 60 m), they all use pulse compression and monopulse angle measurement techniques, the antenna beamwidths are on the order of 1°, and most of them are capable of tracking objects at slant ranges of several thousand miles, with range measurement accuracies on the order of 1–10 m. Further details on these particular radars and phased arrays, pulse compression, and monopulse techniques in general can be found in [1]–[3]. This paper will discuss some aspects of the design of Kalman tracking filters for such radars. Although the discussions are applicable to radar tracking in general, they reflect the experiences of the authors with the several large, long-range phased array radars designed and built at the Raytheon Company, which constitute the majority of the systems in Table I. These are exemplified by the radars shown in Fig. 1(a)–(d).

Our presentation begins with a tutorial on ill-conditioning (Section II), which also includes an analysis that explains two rather common types of filter divergence in applications of this type. Although this analysis is elementary, it provides considerable insight into these phenomena. This is followed in Section III by a discussion of the special coordinate systems used to represent the Kalman filter error covariance matrices. These so-called "covariance coordinates" include range-velocity Cartesian coordinates (RVCC), radar principal Cartesian coordinates (RPCC), and track-oriented Cartesian coordinates (TOCC). Two of these coordinate systems (RPCC and RVCC) were initially developed by Brown and others at IBM [7], although numerous refinements and modifications have been made for the applications in Table I. Section IV considers some computational aspects of these filters, and we conclude in Sections V and VI with a brief review of certain nonlinear aspects of Kalman filtering in applications such as those in Table I. Although the uncertain origin of radar observations [26]–[28] is an important problem in systems such as those in Table I, there is insufficient space to discuss this topic here.

The basic reason for introducing special coordinate systems for representing the Kalman filter error covariance matrix (Section III) is to allow a decoupling of this matrix without suffering a significant loss of state vector estimation accuracy. Decoupling the error covariance matrix has three benefits: 1) reduction in computational requirements, 2) reduction of ill-conditioning (Section II), and 3) mitigation of the ill effects of certain nonlinearities (Sections V and VI). As will be illustrated in subsequent sections, there is often no noticeable loss of accuracy, and in certain cases, there is a substantial improvement in accuracy. It should be noted, however, that for some applications, even partial decoupling may result in significantly suboptimal performance. (Some examples of performance degradation due to decoupling are given in [37].)

The term "decoupling," as used in this context, refers to the approximation of certain covariance matrix elements as zero. For example, the "fully coupled" covariance matrix

$$P = \begin{bmatrix} P_{11} & P_{12} & P_{13} \\ P_{12}^T & P_{22} & P_{23} \\ P_{13}^T & P_{23}^T & P_{33} \end{bmatrix} \tag{1.1}$$

where the $P_{ij}$ are nonzero submatrices, might be reduced to a "partially coupled" matrix by approximating $P_{13}$ and $P_{23}$ by zero matrices. It may be further reduced to a "decoupled" matrix by also letting $P_{12}$ be zero.

The decoupling defined above and the special coordinate systems described in Section III all refer to the error

Manuscript received March 17, 1982; revised August 26, 1982.

F. E. Daum is with the Equipment Division, Raytheon Company, Wayland, MA 01778.

R. J. Fitzgerald is with the Missile Systems Division, Raytheon Company, Bedford, MA 01730.

0018-9286/83/0300-0269$01.00 

TABLE I
LARGE PHASED ARRAY RADARS

| Radar System | Manufacturer of Radar | Operating Frequency | Kalman Filter Characteristics | | |
|---|---|---|---|---|---|
| | | | Dimension of State Vector | Degree of Coupling of Covariance Matrix | Coordinate System For Covariance Matrix |
| AN/FPS-85 | Bendix | UHF | 7 | Full* | Standard Cartesian |
| MSR | Bell Labs/Raytheon | S-Band | 6 or 7 | Partial | RVCC |
| PAR | Bell Labs/GE | UHF | 6 | Decoupled | RPCC |
| Site Defense | McDonnell-Douglas/GE | | 7 | Partial | RVCC |
| Cobra Dane | Raytheon | L-Band | 9 | Decoupled | RPCC |
| PAVE PAWS (Sites I & II) | Raytheon | UHF | 6 | Partial | RVCC/CR |
| Cobra Judy | Raytheon | | | | |

*Modification to RVCC under consideration.

covariance matrix rather than the state vector itself. The prediction of the state vector from one time to the next is generally performed in a Cartesian coordinate system fixed with respect to the radar. The differential equations used to predict the state vector include gravity, Coriolis and centrifugal accelerations due to earth rotation, and also (if needed for a particular application or flight regime) drag, lift, and thrust acceleration. There is no "decoupling" of the equations of motion used to represent or predict the state vector.

## II. Ill-Conditioning in Kalman Filters

Numerical analysts have been keenly aware of the phenomenon known as "ill-conditioning" in connection with matrix inversion for many years (see [10]–[12]). Least squares problems generally give rise to particularly ill-conditioned matrix inversion problems, owing to the redundancy of the data being processed. Considering that a Kalman filter is simply a recursive solution to a certain weighted least squares problem, it is not surprising that Kalman filters tend to be ill-conditioned. An awareness of ill-conditioning of Kalman filters was achieved soon after the first nontrivial applications [13] and [14]. A particularly fine exposition of this topic is given in [4] and [15]; the following material is intended to complement and illuminate the discussion in these two references. Also, it is interesting to compare Kalman's comments in [5], concerning ill-conditioning in optimal control problems, to our analysis.

The first problem to overcome is defining the notoriously elusive term "ill-conditioning." We will do this in the context of solving simultaneous linear equations, which will be adequate for our purposes. Roughly speaking, we say that the problem of solving the linear equation $Ax = b$ for the vector $x$ is "ill-conditioned" if "small" fractional errors in the $n \times n$ matrix $A$ or the vector $b$ result in "large" fractional errors in $x$. The fractional errors in $x$, $A$, and $b$ are $\|\Delta x\|/\|x\|$, $\|\Delta A\|/\|A\|$, and $\|\Delta b\|/\|b\|$, respectively, in which $\Delta x$, $\Delta A$, and $\Delta b$ denote the errors in $x$, $A$, and $b$, $\|x\|$ is the norm of $x$, and $\|A\|$ is the corresponding matrix norm induced by the vector norm (see [12, pp.

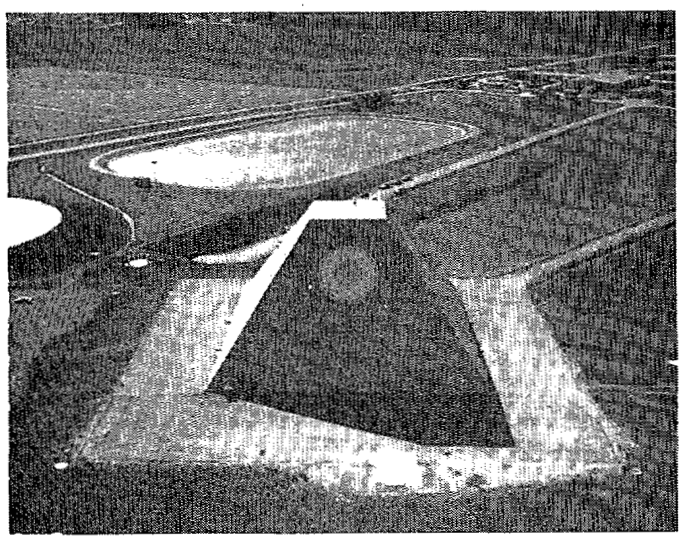

(a)

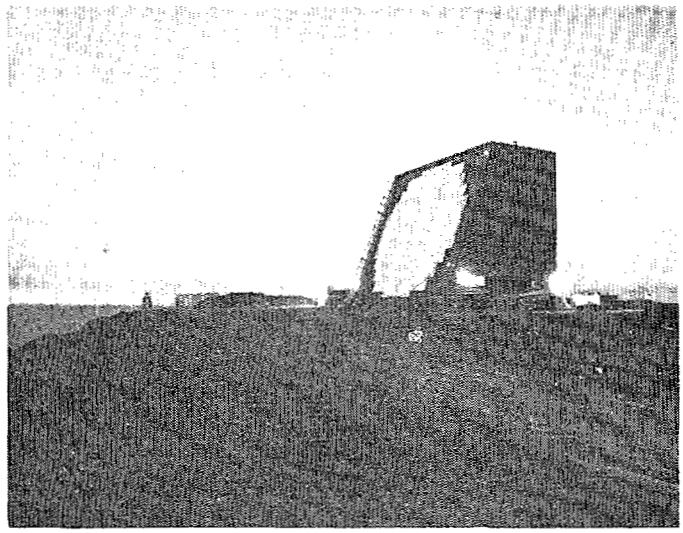

(b)

Fig. 1. (a) Missile site radar (MSR) S-band phased array radar, designed for tracking of reentry vehicles and Spartan missiles in Safeguard ballistic missile defense system. (b) Cobra Dane (AN/FPS-108) L-band phased array radar, designed for collection of data (exoatmospheric) on flight tests of foreign missile systems (also satellite tracking and ICBM early warning).

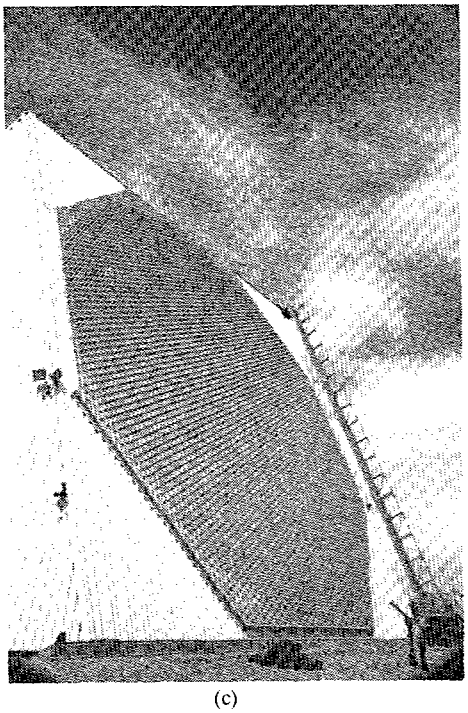

(c)

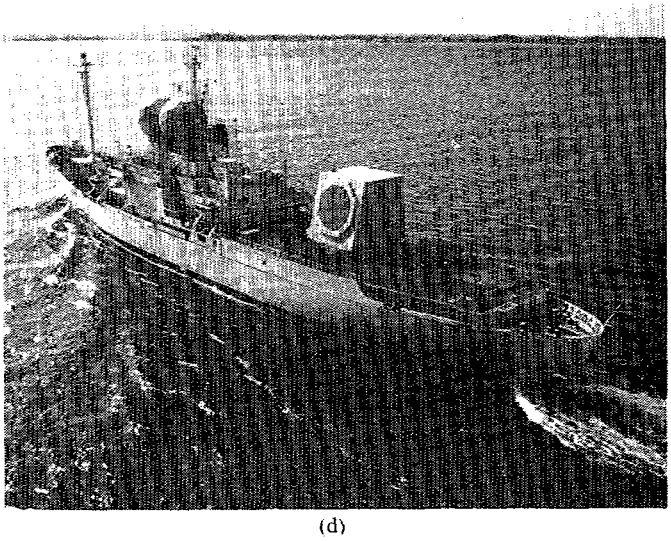

(d)

Fig. 1. (*Continued.*) (c) PAVE PAWS (AN/FPS-115) solid-state UHF phased array radar, designed for early warning of submarine-launched ballistic missiles (also satellite tracking). (d) Cobra Judy (AN/SPQ-11) shipboard phased array radar, designed for collection of data on tests of foreign missile systems (also satellite tracking).

763–771]). Usually we think of the errors in $A$ and $\boldsymbol{b}$ arising from the finite word length in digital computers, although these errors can arise from other sources (e.g., modeling the equations of motion and linearization); scaling and bias errors in an analog computer implementation would qualify as well. Various vector norms are possible, but for this discussion, we will consider only the standard Euclidean norm. The corresponding matrix norm is $\|A\| = \sqrt{\lambda_{\max}(A^TA)}$ in which $\lambda_{\max}(\cdot)$ denotes the largest eigenvalue of $(\cdot)$. At this point, the term "ill-conditioning" is still rather vague, owing to the lack of a rule to determine when to call $\|\Delta x\|/\|x\|$ "large." If fact, the threshold of "largeness" depends on the specific application and the particular norms involved.

The reason that we only need to consider the ill-conditioning of the linear equation $Ax = \boldsymbol{b}$ is that the Kalman filter corrector equation has precisely this form. In particular, one standard form of the state vector corrector equation

$$\hat{x} = \bar{x} + MH^T(HMH^T + R)^{-1}(z - H\bar{x}) \tag{2.1}$$

is mathematically equivalent to

$$(M^{-1} + H^TR^{-1}H)\hat{x} = M^{-1}\bar{x} + H^TR^{-1}z \tag{2.2}$$

which is of the form $Ax = \boldsymbol{b}$ if we make the following identifications:

$$A = M^{-1} + H^TR^{-1}H \tag{2.3}$$

$$\boldsymbol{b} = M^{-1}\bar{x} + H^TR^{-1}z. \tag{2.4}$$

In the above, $\hat{x}$ and $\bar{x}$ denote the corrected and predicted state vectors, respectively; $R$ is the $m \times m$ measurement error covariance matrix; $M$ is the $n \times n$ error covariance matrix of $\bar{x}$; $z$ is the measurement vector ($z = Hx + v$) where $x$ is the true state vector; and $v$ is the measurement noise vector. With this formulation, the vector $\boldsymbol{b}$ itself is the sum of two terms, each of which involves matrix inversions. Consequently, we must consider the conditioning of the three matrices $A$, $M$, and $R$ in order to determine the overall conditioning of the Kalman filter corrector equation. Our focus here is different from other treatments of Kalman filter ill-conditioning which concentrate on numerical errors in the nonlinear covariance matrix equations [9], [13], [22].

Having defined the concept of ill-conditioning, we are now at a point to define a precise mathematical bound [12, p. 809]

$$\frac{\|\Delta x\|}{\|x\|} \leqslant \frac{c(A)}{1 - \|\Delta A\|\|A^{-1}\|}\left[\frac{\|\Delta \boldsymbol{b}\|}{\|\boldsymbol{b}\|} + \frac{\|\Delta A\|}{\|A\|}\right] \tag{2.5}$$

in which $c(A) = \|A\|\|A^{-1}\|$ is called the "condition number." The bound (2.5) is valid under the assumption that $\|\Delta A\|\|A^{-1}\| < 1$, and the norm is such that $\|I\| = 1$ where $I$ is the identity matrix. For obvious reasons, in most interesting practical applications, $\|\Delta A\|\|A^{-1}\|$ is much less than unity, and therefore the condition number is the key parameter. If $A$ is a real symmetric matrix, then the condition number is

$$c(A) = \frac{\lambda_{\max}(A)}{\lambda_{\min}(A)} \tag{2.6}$$

for the Euclidean vector norm considered here. If $c(A)$ is large, then the problem $Ax = \boldsymbol{b}$ may be ill-conditioned, but because (2.5) is only an upper bound, $Ax = \boldsymbol{b}$ might be well-conditioned. In fact, one of the main goals of this paper (as well as [9]–[17]) is to show how to make $Ax = \boldsymbol{b}$ well-conditioned despite enormous values of $c(A)$. The failure to recognize this point is very common (e.g., [5, pp. 27–28]). The bound (2.5) can be extremely pessimistic, depending on the exact form of $A$. For example, if $A$ is the matrix

$$A = \begin{bmatrix} 10^{100} & 0 \\ 0 & 1 \end{bmatrix}, \tag{2.7}$$

then $c(A) = 10^{100}$, but the problem $Ax = b$ is not ill-conditioned at all. This and other defects in the classical definition of condition number have led to alternative definitions (e.g., [7], [15], and [18]), but we will be content with (2.6). Also, with some care, one can define a condition number for the solution of nonlinear problems [19]; however, as indicated earlier, we do not need such a generalization to analyze the Kalman filter corrector equation.

Using (2.5) and (2.6), we can now analyze the (potential) ill-conditioning of Kalman filters. In particular, assuming that $M$ is positive definite, and using the convexity of $\lambda_{max}(\cdot)$ as a function of $(\cdot)$ and the concavity of $\lambda_{min}(\cdot)$ [8, p. 72], it is easy to show that

$$c(A) \leqslant \frac{\lambda_{max}(M^{-1}) + \lambda_{max}(H^T R^{-1} H)}{\lambda_{min}(M^{-1}) + \lambda_{min}(H^T R^{-1} H)} \tag{2.8}$$

in which $A$ is given by (2.3). In some applications, the ill-conditioning is so severe that $M$ eventually fails to be positive definite (e.g., [6]), in which case (2.8) is invalid. Moreover, if $M$ is not positive definite, then the filter is likely to be unstable, and the error in $\hat{x}$ will be unbounded. In any case, (2.8) is a valid bound before $M$ loses positive definiteness; it follows from (2.8) that

$$c(A) \leqslant \frac{1/\lambda_{min}(M) + \lambda_{max}(H^T R^{-1} H)}{1/\lambda_{max}(M) + \lambda_{min}(H^T R^{-1} H)}. \tag{2.9}$$

For the majority of practical applications, including all of those listed in Table I, the measurement matrix $H$ has rank less than $n$, and therefore $\lambda_{min}(H^T R^{-1} H) = 0$. It follows from (2.9) and (2.6) that

$$c(A) \leqslant c(M) + \lambda_{max}(M)\lambda_{max}(H^T R^{-1} H). \tag{2.10}$$

If $H$ has rank $n$, then (2.10) is still valid, but is more pessimistic. Combining (2.10) and (2.5), and assuming that $\|\Delta A\|\|A^{-1}\|$ is much less than unity, yields the main result of this (approximate) analysis:

$$\frac{\|\Delta \hat{x}\|}{\|\hat{x}\|} \leqslant \left[c(M) + \lambda_{max}(M)\lambda_{max}(H^T R^{-1} H)\right] \cdot \left[\frac{\|\Delta A\|}{\|A\|} + \frac{\|\Delta b\|}{\|b\|}\right] \tag{2.11}$$

in which $A$ and $b$ are given by (2.3) and (2.4), respectively. Referring to (2.4), the errors in $b$ arise principally from errors in $\bar{x}$, $M$, and $H$, and to a lesser extent from errors in $z$ and $R$. Note that radar measurement noise should not be considered a source of error in $z$ because $z$ is defined as $Hx + v$, in which $v$ is the noise-induced error. A further application of (2.5) to (2.4) will result in a bound on $\|\Delta b\|/\|b\|$ which explicitly displays its dependence on $c(R)$ and $c(M)$. We shall not pursue this analysis here because (2.11) is sufficient for our immediate purposes; it is interesting to note, however, that such an analysis can produce a bound that is quadratic in $c(M)$. It should be emphasized that (2.2) is not the form of the Kalman filter corrector equation used in most practical applications because its computation generally requires many more operations than the form given in (2.1). Nevertheless, the error bound derived here (2.11) is obviously still valid. The only question is: how tight a bound is (2.11) if (2.1) is used rather than (2.2)? Some insight into this question is derived from the following comments. In particular, [21, pp. 470–479] and [1, p. 371] indicate that, based on practical experience, the computation of $A^{-1}$ via (2.3) is much better conditioned than the mathematically equivalent form $A^{-1} = M - MH^T(HMH^T + R)^{-1}HM$ deduced from Schur's matrix inversion formula. This is true in spite of the fact that the former method requires, in general, many more operations than Schur's alternate method. This suggests that, in general, (2.11) is a tight bound, except for the basic defects in (2.6) noted earlier. This discussion also illustrates the error in the popular notion that fewer operations imply smaller error. (For example, see [5, p. 40].) Other counterexamples to this idea include iterative improvement [12, pp. 831–833] and the so-called Joseph form of the covariance update equation [9, pp. 7, 84]. Moreover, these examples show that ill-conditioning is not related to the number of operations in a simple way, but rather a much more subtle and powerful mechanism is at work.

We will now use (2.11) to interpret a number of results reported in the literature and/or experienced in some of the applications in Table I. First, errors in $A$ and $b$ will be propagated strongly in the initial phase of track when $\lambda_{max}(M)$ may be large; this is especially so immediately after an exceptionally accurate radar measurement because $\lambda_{max}(H^T R^{-1} H)$ would be large in this case. An example of this well-known effect is reported in [6, p. 32]. Second, a result often reported in the literature (e.g., [13], [16], [41]) is the divergence of the Kalman filter after an extended period of tracking. In this case, $\lambda_{max}(M)$ should be relatively small, and therefore the source of difficulty evidently lies in the term involving $c(M)$. The condition number of $M$ can become enormous as the ostensible accuracy of the state vector estimate (as measured by $M$) improves. To gain some insight into this, consider the simple Kalman filter defined by $H = [1,0]$, $R$ = constant, with no *a priori* data and no process noise modeled, and the state transition matrix

$$\Phi = \begin{bmatrix} 1 & T \\ 0 & 1 \end{bmatrix} \tag{2.12}$$

in which $T$, the time between measurements, is a constant. For this example, it is well known [20] that

$$M = \begin{bmatrix} 2(2k-1) & 6 \\ 6 & 12/(k-1) \end{bmatrix} \frac{R}{k(k+1)} \tag{2.13}$$

in which $k$ is the number of measurements and $T = 1$ is assumed without loss of generality. It can be shown, using (2.13), that $c(M) = \lambda_{max}(M)/\lambda_{min}(M)$ is unbounded for increasing $k$. Moreover, both $\lambda_{max}(M)$ and $\lambda_{min}(M)$ approach zero for this example. Therefore, contrary to the untutored intuition, as the Kalman filter thinks the estimate of $\hat{x}$ becomes more and more accurate, the error

TABLE II
METHODS TO REDUCE ILL-CONDITIONING

| | Method | Comment |
|---|---|---|
| 1. | Approximate decoupling of covariance matrix | See Section III. |
| 2. | Diagonalization of covariance matrix | e.g. Gram-Schmidt technique used in adaptive arrays (Ref. 23). |
| 3. | Covariance matrix factorization | See Refs. 6, 9 and 22. |
| 4. | Lower bound main diagonal elements of covariance matrix | Encourages positive definite covariance matrix, but does not guarantee it. |
| 5. | Introduce or increase process noise | Makes plant model controllable. |
| 6. | Tikhonov regularization (also called ridge analysis) | Implicit in Kalman-Wiener filter formulation; see Ref. 11. |
| 7. | Extra precision arithmetic (e.g. double precision) | For real-time applications such as those in Table 1, this would impose a significant memory and throughput burden. |
| 8. | Iterative improvement | See Refs. 10 and 12; implicit in some iterated least squares methods. |
| 9. | Joseph's stabilized form of covariance update equation | See pp. 25 and 31 of Ref. 6 for caveats on this method. |
| 10. | Updating the covariance matrix with a sequence of scalar measurements | See Refs. 16 and 17; avoids non-scalar matrix inversion. |
| 11. | Preferred order of processing scalar measurements | In Ref. 24 this technique is shown to reduce errors due to nonlinearities, but it should also reduce ill-conditioning for certain applications. |
| 12. | Scaling or equilibration of covariance matrix | See Refs. 10 and 12. |
| 13. | Rearrangement of filter equations to preserve precision | See pp. 91-96 of Ref. 9. |
| 14. | H matrix of rank n | Usually cannot be achieved in practical applications. |

propagation given in (2.11) becomes arbitrarily large. This is precisely the phenomenon described in [13] and [16] among others. Finally, it is useful to note that $M$ is (theoretically) positive definite for all finite $k$; moreover, the pair $(H, \Phi)$ defines an observable system for $k \geq 2$ [20], although the plant model is obviously uncontrollable. The Kalman filter in this example also happens to be asymptotically unstable, having both poles on the unit circle. (Recall that Kalman's theorem relating controllability and observability to filter stability [45] allows, but does not imply, asymptotic instability of the filter in this case.)

As a result of this phenomenon, it has become standard engineering practice to model some process noise in the Kalman filter design (to make the plant model controllable) and/or explicitly bound the main diagonal elements of $M$ from below. With these safeguards, $\lambda_{\min}(M)$ cannot become arbitrarily close to zero, and $c(M)$ is bounded from above. Nevertheless, it is well known that these ad hoc devices are insufficient to prevent ill-conditioning in many applications. The situation is particularly severe in radars such as those listed in Table I, in which $\lambda_{\max}(M)$ is approximately the variance of position estimation error normal to the radar line of sight, whereas $\lambda_{\min}(M)$ is typically the variance of range-rate estimation error. Under these circumstances, $c(M)$ increases quadratically in track time, and can easily attain values of $10^7$ or more [15] before the process noise or lower bounds on the main diagonal elements of $M$ take effect. In view of this, further steps to reduce ill-conditioning are usually required. Table II is a list of the most common methods to mitigate ill-conditioning. These techniques can be used singly or in various combinations. For example, in one of the applications listed in Table I, we have used Methods 1, 4, 5, 6, 9, and 13 in one Kalman filter. Also, it may be useful to note that Methods 1 and 3 are compatible. The method of decoupling the covariance matrix (Section III) has the advantage over all the others of dramatically reducing ill-conditioning, as well as significantly decreasing the number of operations required in real time. Table III quantifies these considerations for a typical application in Table I. Table III also indicates the problems associated with too much decoupling. The results in Table III are based on well-tuned process noise models for each filter with 60-bit floating-point arithmetic used for all computations. Also, the track rates, average signal-to-noise ratio, radar cross-section fluctuation statistics, duration of track, missile trajectories, radar model, etc., were identical for all three filters. Table IV gives some further details of the comparison between the fully coupled and partially coupled filters for three different missile trajectories.

In order to understand why approximate decoupling (Method 1) reduces ill-conditioning, one should think of this method as a step in the direction of diagonalization of the covariance matrix (Method 2 in Table II). In fact,

TABLE III
COMPARISON OF THREE SIX-STATE KALMAN FILTERS

| Degree of Coupling | Full | Partial | Decoupled |
|---|---|---|---|
| Coordinate system for covariance representation | Standard Cartesian | RVCC | RPCC |
| Normalized one-sigma impact prediction errors for various missile trajectories | 1.0 to 2.0 | 0.6 to 1.0 | 0.6 to 4.0 |
| Number of operations per measurement | 3650 | 1750 | 840 |

TABLE IV
COMPARISON OF FULLY COUPLED AND PARTIALLY COUPLED SIX-STATE KALMAN FILTERS

| Local Flight Path Angle of Missile | Angle Off Array Boresight | Trajectory Orientation Relative to Radar | Normalized One-Sigma Impact Prediction Errors | |
|---|---|---|---|---|
| | | | Fully Coupled Filter | Partially Coupled Filter |
| $60^0$ | $45^0$ | Crossing | 1.4 | 1.0 |
| $30^0$ | $60^0$ | Radial | 2.0 | 1.0 |
| $30^0$ | $0^0$ | Radial | 1.0 | 0.6 |

Method 1 is a type of approximate block diagonalization. It is obvious that a diagonal matrix is not ill-conditioned at all. Diagonalization is a very old and well-known technique in least squares problems. The use of orthogonal polynomials rather than the standard basis $(1, x, x^2, \cdots)$ to perform least squares curve fitting is an application of this idea, which is associated with such names as Legendre, Laguerre, Hermite, etc. In the context of dynamical systems, it is known that the eigenvalues of the transition matrix $(\Phi)$ of a linear system are least sensitive to numerical errors if $\Phi$ is realized in diagonal form [34].

Finally, it should be noted that some progress has been made towards formulating the precise connection between decoupling and ill-conditioning in [44, ch. II].

As an illustration of this idea applied to covariance matrices, consider the simple example

$$P_1 = \begin{bmatrix} 1 & 1-\epsilon \\ 1-\epsilon & 1 \end{bmatrix} \tag{2.14}$$

where $0 < \epsilon \ll 1$. $P_1$ has positive eigenvalues $\lambda_1 = 2-\epsilon$ and $\lambda_2 = \epsilon$. In a computer of finite word length (using floating-point or well-scaled fixed-point arithmetic), roundoff errors will tend to produce fractional errors of a particular size in the variables. It is evident from (2.14) that a small fractional error in the off-diagonal element will be equivalent to a large fractional error (or even a sign error) in $\epsilon$, and hence in the smaller eigenvalue $\lambda_2$. Thus, the rounded-off matrix may have eigenvalues greatly in error, and may even lose its positive definiteness. In contrast, if principal coordinates are utilized so that the matrix has the diagonal form

$$P_2 = \begin{bmatrix} 2-\epsilon & 0 \\ 0 & \epsilon \end{bmatrix}, \tag{2.15}$$

then fractional errors of moderate magnitude will not seriously alter the eigenvalues or the essential properties of the matrix.

The same ideas can be presented graphically by construction of a Mohr circle [42] to represent the covariance matrix of (2.14) and (2.15). The circle is shown in Fig. 2. In general, the circle representing the covariance matrix $P$ of a random vector in the $xy$ plane is drawn on a diameter defined by the two points $X(P_{11}, -P_{12})$ and $Y(P_{22}, +P_{12})$. Then if the coordinate axes are rotated through an angle $\theta$, a rotation of the diameter through an angle $2\theta$, in the same sense, yields a new diameter whose end points represent the elements of the transformed covariance matrix. In the present case, the matrix $P_1$ is represented by the points $X_1(1, -1+\epsilon)$ and $Y_1(1, 1-\epsilon)$. A rotation through 45° (90° on the Mohr circle) brings us to the principal-axis representation of (2.15), represented by the points $X_2(2-\epsilon, 0)$ and $Y_2(\epsilon, 0)$. It is evident from the figure that small fractional errors in the coordinates of $X_1$ and $Y_1$ may produce large errors in the smaller eigenvalue (the abscissa of $Y_2$), even to the extent of destroying positive definiteness (in which case the abscissa becomes negative). No such problem exists when the matrix is represented as in (2.15) (i.e., represented directly by the coordinates of $X_2$ and $Y_2$).

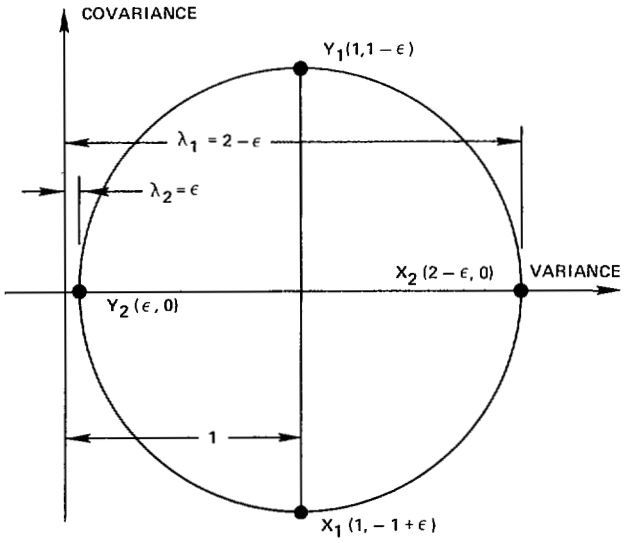


Fig. 2. Mohr circle representation of the covariance matrix of (2.14) and (2.15).

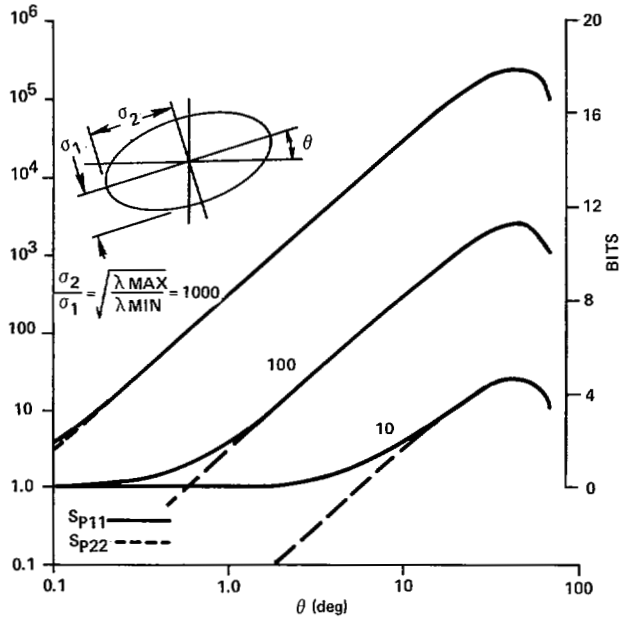


Fig. 3. Eigenvalue sensitivities for a 2×2 covariance matrix.

The above concepts can be quantified by computing the sensitivities (partial derivatives) of the smallest eigenvalue

$$\lambda_{\min} = \frac{P_{11}+P_{22}}{2} - \sqrt{\left(\frac{P_{11}-P_{22}}{2}\right)^2 + P_{12}^2} \quad (2.16)$$

with respect to the individual covariance-matrix elements $\partial\lambda_{\min}/\partial P_{ij}$. In order to deal with relative errors, we may normalize these derivatives to yield sensitivity functions of the form

$$S_{P_{ij}} = \frac{P_{ij}}{\lambda_{\min}} \frac{\partial \lambda_{\min}}{\partial P_{ij}}. \quad (2.17)$$

For 2×2 covariance matrices with high flattening ratio $\sigma_2/\sigma_1$, Fig. 3 shows the extreme sensitivities which can result from even small misorientation angles $\theta$ between the coordinate axes and the principal axes. (The right-hand scale, expressed in powers of two, can be interpreted as the number of bits of precision lost in $\lambda_{\min}$ for a 1-bit error in $P_{ij}$.)

It is interesting to note that if $P$ is expressed in the factorized form $P = SS^T$ ($S$ triangular), all of the sensitivities $S_{Sij}$ remain small, regardless of $\theta$. Such a statement cannot be made, however, when we employ the factorization $P = UDU^T$ ($D$ diagonal, $U$ triangular and unitary). Furthermore, scaling of the covariance matrix (so that all of its diagonal elements are equal) does not change any of these conclusions.

Although the applications discussed here all involve computers of considerable word length, short word-length implementations (for example, 16 bits) are common. The result is larger fractional errors due to roundoff, and hence an increase in the importance of ill-conditioning, as demonstrated by the above examples.

## III. Decoupled Tracking

In using covariance coordinates for tracking filter decoupling, the basic objective is to perform the covariance computations in coordinates which are, as nearly as possible, principal coordinates of the error covariances. If the covariance matrix can be visualized as representing an error ellipsoid (which is easily done, for example, if it represents only position errors in three-dimensional space), then the appropriate coordinate axes are the principal axes of this ellipsoid.

Tracking problems are usually more amenable to this technique than are estimation problems in general because it is often possible to predict, quite readily, which coordinate axes will produce the desired result. For example, when the target dynamics exhibit no significant directional properties, one might immediately surmise that the principal axes of the measurement error ellipsoid would constitute an appropriate axis system in which to perform the covariance computations. Provided that these axes do not change their orientation at an appreciable rate, the resulting estimation errors in each axis will be largely uncoupled from those in the other axes. If, for example, the covariance matrix is a 6×6 matrix representing estimation errors in position and velocity in three Cartesian coordinate directions, it can be expected that the only significant off-diagonal elements will be those which represent cross correlations between position and velocity errors in the same axis. If the other (small) elements are neglected, the resulting matrix can be represented as three distinct uncoupled 2×2 matrices. If we use the rough rule of thumb that the computational cost of covariance propagation is proportional to $n^3$ (where $n$ is the number of states), we find that the computation has been reduced by a factor of $6^3/(3\times 2^3) = 9$.

Even when Kalman filters (i.e., filters which use covariance propagation for gain determination) are not utilized,

TABLE V
APPROACHES TO DECOUPLED TRACKING

| Coordinate System | Number of States | Applications | Examples |
|---|---|---|---|
| RPCC (Radar Principal Cartesian Coords) | 3,3,3 or 2,2,2 or 3,2,2 | Meas. errors (ME) highly directional; LOS rotation slow relative to filter memory | Aircraft or missiles in the atmosphere |
| TOCC (Track-Oriented Cartesian Coords) | 3,3,3 or 2,2,2 or 2,3,3 | Dynamic errors (DE) highly directional (or ME directional along velocity); LOS rate slow | Air traffic control |
| RVCC (Range-Velocity Cartesian Coords) | 6,3 or 4,2 or 5,2 | ME and DE both highly directional; LOS rate slow | Reentry vehicles |
| RVCC/CR (RVCC with Covariance Rotation) | 6,3 or 4,2 | LOS rate significant relative to filter memory (perhaps because of long memory due to small DE) | Exoatmospheric missiles, satellites, space vehicles |

the concept of covariance coordinates facilitates decoupling of the tracking problem, and indeed makes possible the successful application of simple precomputed-gain filters, such as those of the so-called "$\alpha\beta\gamma$" or "*ghk*" type [29]. In this sense, the concept, in its simplest form, is implicit in many of the approaches commonly used today for decoupled tracking.

In more complex situations, such as those involving directional target dynamics or a rapidly rotating line of sight, the concept must be modified appropriately. This leads to a family of related decoupling techniques which have repeatedly proven their effectiveness in various applications over the past decade. These concepts were originally developed for the Safeguard system where they were utilized for tracking Sprint missiles and reentry vehicles [7], [30]; they have since been applied to a variety of other systems, and the results of some of these applications are discussed here.

Four classes of decoupled tracking schemes are described briefly below. Table V provides a summary of the four approaches, and outlines the conditions under which each may be appropriate.

### *RPCC Filters*

Radar principal Cartesian coordinates (RPCC's) are defined as the directions of the principal axes of the error ellipsoid of the radar position measurements. Such an ellipsoid is depicted in Fig. 4. In the case of a phased array radar, it is customary to define a set of face ($F$) Cartesian coordinates with the $z_F$ axis normal to the array face and the $x_F$ and $y_F$ axes in the face. Then the target position vector in face coordinates is given by

$$\boldsymbol{X}_F = \begin{bmatrix} x_F \\ y_F \\ z_F \end{bmatrix} = \begin{bmatrix} ru \\ rv \\ rw \end{bmatrix} \tag{3.1}$$

where $r$ is the range and $u$, $v$, and $w$ are the direction cosines of the range vector or line of sight (LOS), related by $u^2 + v^2 + w^2 = 1$ or $w = \sqrt{1 - u^2 - v^2}$.

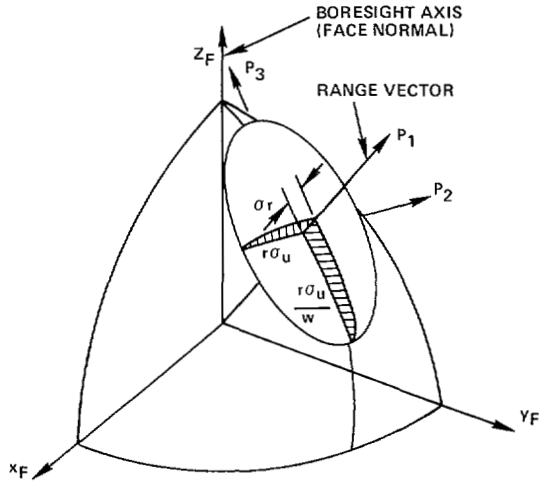


Fig. 4. Measurement error ellipsoid and RPCC coordinates for a phased array radar.

The quantities normally measured by the radar are $r$, $u$, and $v$, and their measurement errors are characterized by a diagonal covariance matrix $R_M = \text{diag}(\sigma_r^2, \sigma_u^2, \sigma_v^2)$. When $\sigma_v = \sigma_u$ (as is generally the case for a circular or square array), it can be shown that the RPCC (or "$P$") axes are oriented as shown. The $P_1$ axis lies along the range vector, $P_2$ is parallel to the radar face plane, and $P_3$ lies in the plane of $P_1$ and the face normal. In this coordinate system, the measurement error covariance matrix is

$$R_P = [PF][FM]R_M[FM]^T[PF]^T \tag{3.2}$$

where $[PF]$ is the transformation matrix from $F$ to $P$ coordinates,

$$[PF] = \begin{bmatrix} u & v & w \\ -v/a & u/a & 0 \\ -uw/a & -vw/a & a \end{bmatrix} \tag{3.3}$$

with $a = \sqrt{1 - w^2} = \sqrt{u^2 + v^2}$, and $[FM]$ is the linearized transformation matrix from measurement ($ruv$ or $M$) coor-

dinates to $F$, which may be found by differentiation of (3.1):

$$[FM] = \begin{bmatrix} u & r & 0 \\ v & 0 & r \\ w & -ru/w & -rv/w \end{bmatrix}. \quad (3.4)$$

It is readily verified that (3.2) results in a diagonal measurement-error covariance matrix in the Cartesian $P$ frame, given by

$$R_P = \operatorname{diag}\left(\sigma_r^2, r^2\sigma_u^2, r^2\sigma_u^2/w^2\right). \quad (3.5)$$

If rotations of the line of sight (LOS) can be neglected, and if the dynamic error effects due to unpredictable target motions can be assumed to be approximately the same in all directions (spherically isotropic), then the principal directions for the estimation errors can be assumed to remain along the RPCC axes, and hence covariance computations can be decoupled in these axes.

Such an approach can often be applied successfully to the tracking of airborne targets such as aircraft and missiles, and of sea targets such as ships and submarines. In propagating the three independent covariance matrices, rotation of the line of sight is ignored completely. Significant LOS rates will result in the true error principal directions lagging behind the RPCC system; resulting is a degree of cross coupling and a degradation of performance of the decoupled filter. Furthermore, LOS rotation produces a triangulation effect which can significantly reduce the estimation errors in the cross-range direction; this effect is not usually taken into consideration in the decoupled propagation of the covariance matrices, resulting in an additional loss of performance relative to that of a fully optimum approach.

For these reasons, the fully decoupled RPCC tracker yields near-optimum performance only when the LOS rate is small. In this context, the significance of the LOS rate must be judged in relation to the memory lengths of the filters (i.e., the significant parameter is the LOS rotation per memory length); the governing filter in this regard is the one with the largest measurement errors, and hence the narrowest bandwidth (longest memory), which is usually the filter operating in the cross-range direction rather than the range direction. Furthermore, since filter memory is longer when dynamic errors are small, even small LOS rates can cause performance degradation in cases where the filter's dynamic equations accurately model the target behavior, as is often the case in exoatmospheric tracking.

The above implies that considerable LOS rates can be tolerated as long as the tracking filters have wide bandwidths (i.e., large gains). This has been shown to be the case in the Safeguard application [30] where RPCC filters have been used successfully to track fast-moving Sprint missiles at short ranges.

In many applications (including those described here), the radar measurement error ellipsoid is flattened to an extreme degree, especially at long range. Flattening ratios (ratios of maximum to minimum rms error) of 1000 or more are not uncommon. (By way of comparison, the corresponding ratio of diameter to thickness of an ordinary LP phonograph record is generally in the vicinity of 200.) With such extreme flattening, small changes in LOS angle, if properly accounted for in a fully coupled Kalman filter, can yield drastic reductions in the estimation errors in the cross-range directions. Thus, extreme flattening and significant LOS rotation rates conspire together, in a decoupled filter, to degrade performance from the theoretical optimum.

In contrast to these high flattening ratios, the differences in cross-range rms errors (the two largest axes of the error ellipsoid) are often not very significant. For a circular phased array like those discussed here, their ratio (Fig. 4) is equal to $w = z_F/r$, the cosine of the off-boresight angle of the beam, and generally lies between unity and approximately $1/2$. This difference can often be ignored, and an average value can be used in both cross-range axes so that the same covariance matrix and filter gains can be used in both axes. Since much of the computational burden is normally in the covariance-matrix propagation, this can lead to significant further savings. By the same token, such an assumed circularization of the error ellipsoid means that often any other Cartesian coordinate system, rotated from the RPCC set around the range vector, can be utilized just as well as the original RPCC coordinates. The important thing is that the range direction itself, with its much smaller measurement errors, be retained as one of the coordinate axes.

For application to dish antennas rather than phased arrays, identical considerations apply for filter decoupling. In this case, the $z_F$ axis in Fig. 4 can be interpreted as the antenna's azimuth axis, and the rms measurement errors may be defined somewhat differently. (In particular, a fan-beam radar may have quite different accuracies in the $P_2$ and $P_3$ directions.)

Of course, it is apparent that similar principles would apply if the range errors were much *larger* than the cross-range errors (as they often are in CW radars), in which case the error ellipsoid would be shaped like a cigar rather than a pancake.

### *TOCC Filters*

When the directionality properties of the dynamic errors are much more important than those of the measurement errors, so that the latter may be approximated as isotropic, it may be appropriate to align the filtering coordinate axes with the principal dynamic-error directions. In air traffic control applications where target accelerations are almost entirely normal to the direction of flight, this has led to the use of the TOCC (track-oriented Cartesian coordinates) system for tracking filter decoupling [31]. A similar approach could be appropriate for tracking a reentry vehicle (RV); in this case, variations in the ballistic coefficient (or our lack of knowledge of its magnitude) and atmospheric uncertainties and inhomogeneities result in error propagation predominantly in the direction of the velocity vector.

The appropriateness of the TOCC approach may also result from measurement-error directionality in cases where target-induced measurement errors such as radar glint predominate. Such may be the case, for example, when a homing missile or torpedo nears an elongated target such as an airplane fuselage, a waking RV, or a submarine.

In the TOCC case, of course, it is the target's turn rate, rather than LOS rotation, which is likely to degrade the performance of the decoupled filter.

*RVCC Filters*

In cases where both the measurement errors and dynamic errors are directional in character, in general no single coordinate system will result in complete decoupling. The most common such case is when the measurement accuracy is predominantly in the range direction $\boldsymbol{r}$, while the target velocity direction $\boldsymbol{v}$ is the unique one for dynamic error propagation; this is usually the case, for example, in reentry vehicle tracking [32]. In this case, the plane defined by the $\boldsymbol{r}$ and $\boldsymbol{v}$ vectors is the only one which constitutes a common plane of symmetry for the measurement and dynamic errors. It now becomes appropriate to *partially* decouple the covariance computations in the RVCC (range-velocity Cartesian coordinates) system. This "$V$" coordinate system is usually defined with $V_1$ along the range vector $\boldsymbol{r}$, $V_2$ normal to $V_1$ in the $\boldsymbol{r}$-$\boldsymbol{v}$ plane, and $V_3$ normal to that plane. The unit vectors along the RVCC axes are thus given by

$$\begin{aligned} \boldsymbol{u}_{V1} &= \boldsymbol{u}(\boldsymbol{r}) \\ \boldsymbol{u}_{V2} &= \boldsymbol{u}_{V3} \times \boldsymbol{u}_{V1} \\ \boldsymbol{u}_{V3} &= \boldsymbol{u}(\boldsymbol{r} \times \boldsymbol{v}) \end{aligned} \tag{3.6}$$

and these three vectors constitute the rows of the transformation matrix $[VF]$, from face to RVCC.

The covariance computations for the $V_3$ axis can now be performed independently, while a second coupled covariance matrix is utilized in the $\boldsymbol{r}$-$\boldsymbol{v}$ (or $V_1 - V_2$) plane. Thus, for example, a nine-state filter can be decoupled into a three-state and a six-state filter. For RV tracking in the atmosphere, a two-state (position and velocity) filter is often used in the $V_3$ direction, and a five-state filter (with some function of ballistic coefficient as the fifth state) in the $\boldsymbol{r}$-$\boldsymbol{v}$ plane [7].

The availability of a Doppler (range rate) measurement also makes such a partial filter coupling desirable. Consider, for example, a six-state (position and velocity) tracking filter for which the state corrections are to be computed in the RPCC frame of Fig. 4. Then the appropriate Kalman filter $H$ matrix (the partial derivative matrix of the measurement with respect to the states) contains derivatives of $\dot{r}$ with respect to elements of the state vector

$$\boldsymbol{x} = [r_1 \ r_2 \ r_3 \ v_1 \ v_2 \ v_3]^T. \tag{3.7}$$

Since

$$\dot{r} = \frac{\boldsymbol{r} \cdot \boldsymbol{v}}{\sqrt{\boldsymbol{r} \cdot \boldsymbol{r}}}, \tag{3.8}$$

we have, by differentiation,

$$H = \frac{1}{r^2}\left[(rv_1 - \dot{r}r_1) \ (rv_2 - \dot{r}r_2) \ (rv_3 - \dot{r}r_3) \ rr_1 \ rr_2 \ rr_3\right]. \tag{3.9}$$

Now in RPCC, $r_1 = r$, $r_2 = r_3 = 0$, and $v_1 = \dot{r}$. Hence,

$$H = \left[0 \ \frac{v_2}{r} \ \frac{v_3}{r} \ 1 \ 0 \ 0\right]. \tag{3.10}$$

Thus, the $\dot{r}$ measurement exhibits sensitivities to cross-range position errors in the $P_2$ and $P_3$ directions, as well as to velocity errors in the $P_1$ direction. In general, therefore, all three axes are coupled together, and a fully coupled filter is called for. If we utilize RVCC coordinates, however, then $v_3 = 0$ by definition, and the third axis remains uncoupled from the other two.

Even when a Doppler measurement is not used, a similar situation occurs when a linear-FM (chirp) pulse is utilized because of the range-Doppler coupling effect [33]. The "range" quantity measured is

$$m = r + T_c\dot{r} \tag{3.11}$$

where

$$T_c = T_p \frac{f_0}{f_2 - f_1}. \tag{3.12}$$

$T_c$ is the range-Doppler coupling constant, $T_p$ is the pulse length, $f_0$ is the center frequency of the pulse, and the frequency sweep within the pulse is from $f_1$ to $f_2$. Thus, $(f_2 - f_1)$ is the swept bandwidth, and may be positive (upsweep) or negative (downsweep). For conventional radars, the coupling constant $T_c$ is usually on the order of a few milliseconds or less, but for sensitive long-range phased arrays such as those discussed here, extreme pulse lengths may result in much larger values for $T_c$ (up to 36 s for PAVE PAWS).

*RVCC/CR Filters (with Covariance Rotation)*

In the RPCC and RVCC filters described above, it was tacitly assumed that LOS rotation is ignored in propagating the Kalman filter covariance matrices. The covariance coordinate frame is nonrotating between measurements, but is redefined (with a slightly different orientation) at each measurement time. The filter ignores the effects of these reorientations on the covariance matrices, and simply assumes that the matrices predicted in the old frame are valid in the new. As discussed above, this leads to a loss of performance due to covariance-matrix misorientation and disregard of triangulation effects when the LOS rate is significant.

Since both of these degradation effects are connected with covariance rotations in the plane of LOS rotation, they can be virtually eliminated by utilizing an RVCC filter to preserve covariance coupling in that plane, and performing a small rotational transformation on the in-plane covariance matrix to account for intermeasurement LOS

rotation. The transformation takes the form

$$P' = LPL^T \tag{3.13}$$

where $P$ is the in-plane covariance matrix and (for the case of a $4\times4$ $P$ matrix for two positions and two velocities, for example)

$$L = \left[\begin{array}{cc|cc} \cos\epsilon & \sin\epsilon & 0 & 0 \\ -\sin\epsilon & \cos\epsilon & 0 & 0 \\ \hline 0 & 0 & \cos\epsilon & \sin\epsilon \\ 0 & 0 & -\sin\epsilon & \cos\epsilon \end{array}\right]. \tag{3.14}$$

The LOS rotation angle $\epsilon$ is computed as

$$\epsilon = \frac{\Delta t}{r}(\boldsymbol{u}_{V2}\cdot\boldsymbol{v}) \tag{3.15}$$

where $\boldsymbol{u}_{V2}$ is a unit vector in the direction of the second (in-plane cross-range) axis of the RVCC frame.

In practice, computation can be saved by combining the rotation operation with covariance prediction in the form $(\Phi L)P(\Phi L)^T$ where $\Phi$ is the transition matrix. Small-angle approximations may also be employed.

With the added operation of covariance rotation, the RVCC filter becomes capable of tracking, in near-optimum fashion, in the presence of rapid LOS rotation and extreme directionality in measurements and/or dynamics. The principal remaining obstacle to complete optimality is the possibility of rapid rotation of the $\boldsymbol{r}-\boldsymbol{v}$ plane around the line of sight, such as might occur in the case of a violently maneuvering target. In such cases, it may be necessary to maintain full coupling of the covariance matrix; however, covariance coordinates may still be employed to advantage to reduce ill-conditioning effects. Such an implementation might include the propagation of a fully coupled covariance matrix in RPCC, with covariance rotation around *both* cross-range axes; the resulting algorithm is more costly computationally than a standard fully coupled filter, but the alleviation of ill-conditioning may make this a desirable approach.

### *Performance Comparison*

A typical performance comparison is presented in Fig. 5 in the form of rms position errors from a 25-run Monte Carlo simulation of a reentry vehicle tracking problem. The RV is tracked from 41 km altitude on a flight path inclined at 35°, and passes within 15 km of the radar at an altitude of 6.7 km. Measurements are taken every 0.1 s, with typical accuracies in range and angle; the ballistic coefficient $\beta$ has a correlated random component added to its nominal value.

The standard of comparison is provided by a seven-state fully coupled filter operating in earth-fixed Cartesian coordinates. A decoupled filter in *ruv* coordinates (with the $\beta$ state in the range filter) operates well at small aspect angles (high altitude), but shows considerable degradation when the crossing geometry becomes severe. The difficulty is largely eliminated by the RVCC filter, even without covariance rotation. (With covariance rotation, the degradation due to decoupling could probably be expected to be negligible.)

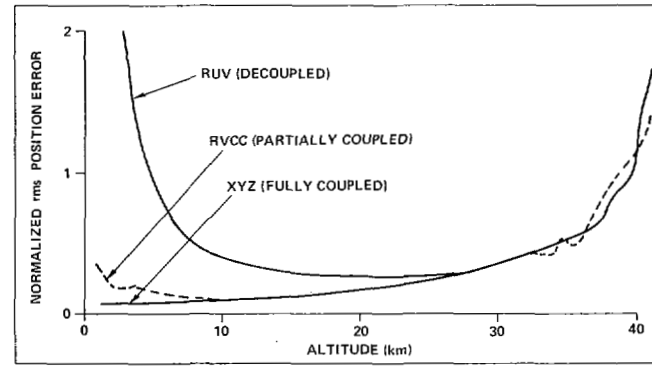


Fig. 5. Performance comparison for three RV tracking filters.

## IV. Implementation Alternatives

The implementation of these decoupled filters is exemplified by the flowchart in Fig. 6, which represents an RVCC filter with covariance rotation. In this particular configuration, the measurement residuals are computed in *ruv*($M$) coordinates and transformed to RVCC where they are multiplied by the gain matrix

$$K_{VV} = P_V H_{VV}^T R_V^{-1} \tag{4.1}$$

to yield state corrections in RVCC, which are then transformed to $F$ before being applied to the state estimates.

The state estimates are propagated in radar face coordinates. Although it is possible to utilize *ruv* coordinates for this portion of the algorithm, Cartesian coordinates are usually preferable because of the less complex differential equations involved and the ease with which these equations can be integrated using simple algorithms [25].

The configuration shown here, in which the gains transform residuals to state corrections in the same decoupled coordinate frame, results in $H$ matrices of a particularly simple form. For a six-state filter (three positions, three velocities) we have, assuming simple position measurements,

$$H_{VV} = \left[\begin{array}{c|c} I & 0 \\ 3\times3 & 3\times3 \end{array}\right]. \tag{4.2}$$

In addition, especially for RPCC filters, this type of configuration sometimes makes possible the use of simple filters with constant or precomputed gains, or highly simplified gain algorithms without covariance propagation.

A variety of other configurations is possible. For example, the residuals may be left in $M$ coordinates and the corrections still generated in $V$, in which case the gain matrix is given by

$$K_{VM} = P_V H_{MV}^T R_M^{-1}. \tag{4.3}$$

In general, the $R$ matrix in the gain equation must be in the

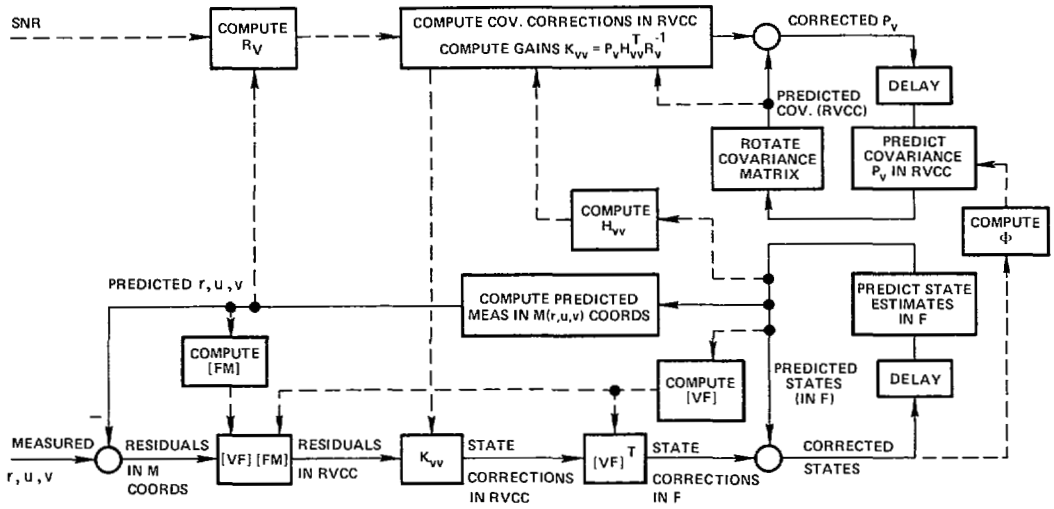


Fig. 6. RVCC decoupled tracker (with covariance rotation).

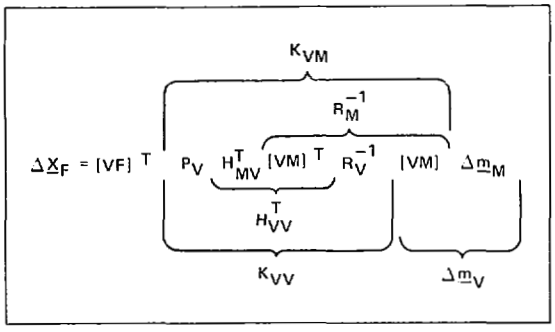


Fig. 7. Alternative interpretations of the state-correction operation.

same coordinates as the residuals to which the gains are to be applied, and the $P$ matrix is in the coordinates in which the state corrections are to be generated. In the example of (4.3), the transformation between $V$ and $M$ is now absorbed into the $H$ matrix, which is related to $H_{VV}$ by

$$H_{MV} = [MV] H_{VV}. \tag{4.4}$$

The relationship between the two approaches is depicted in Fig. 7, in which $\Delta \boldsymbol{m}$ represents the residual vector and $\Delta \boldsymbol{x}$ the state-correction vector. (In Figs. 6 and 7, the matrix $[VF]^T$, which transforms the state corrections from $V$ to $F$, must be regarded as an expanded version of the $3 \times 3$ matrix generated by (3.6), enlarged to the dimension of the state vector.)

Another possible modification is to transform the measurements directly to $F$ coordinates and perform the state differencing (form the residuals) in $F$. This procedure alters the effects of measurement nonlinearities, although not necessarily in a beneficial way. An approach which does appear to be beneficial in dealing with nonlinearities is that of [24]: sequential (rather than simultaneous) measurement processing is used, with the range measurement being processed last. (The state estimates after angle measurement processing are used to redefine the filtering coordinates, and in computing the range residual.)

## V. Nonlinearities

All of the Kalman filters listed in Table I are based on linearizing the differential equations of motion and the measurement equations to compute the $\Phi$ and $H$ matrices. Errors in this linearization process lead to degraded tracking performance to some extent. Moreover, the basic Kalman filter theory assumes Gaussian state estimation error distributions, an assumption that is only approximate for the applications of interest here. Even if the measurement noise and the process noise were both Gaussian, the resulting errors in $\hat{x}$ would be non-Gaussian, owing to the nonlinearities noted above. These nonlinearities can lead to biases, instability, and/or filter divergence. Many methods have been developed to mitigate these effects, a number of which are summarized in Table VI. Several of these techniques were used in early tracking filter simulations for some of the applications in Table I with very poor results. In particular, Methods 1 and 2 in Table VI produced tracking errors in position and velocity that were larger than without these techniques. The poor performance of the second-order filter may be related to the theoretical errors noted in [38], and some insight into the failure of single-stage iteration (i.e., relinearization using an improved state vector estimate) is given in [43]. Although Method 3 in Table VI has worked well in one radar application not listed in Table I, this batch technique is reported to be inferior (as measured by the radius of convergence) to a standard Kalman filter in certain other applications [40]. Concerning Method 4 of Table VI, [32] and [37] indicate possible advantages of *ruv* coordinates over Cartesian coordinates because of the linearity of the measurements in *ruv*. However, [15] and [25] indicate that such is not necessarily the case. In [25], a minor modification to the initialization procedure for the Cartesian filter eliminated large bias-like errors, and resulted in performance virtually identical to that of an *ruv* filter. We have not applied Methods 5, 6, and 7 to radar tracking problems, but they appear to be promising.

TABLE VI
METHODS TO MITIGATE NONLINEARITIES

| Method | Comments |
|---|---|
| 1. Second Order Filter | See Ref. 37 and 38; may produce results worse than the first order filter. |
| 2. Single-Stage Iteration | See Refs. 37 and 43; may produce results worse than no iteration. |
| 3. Batch Least Squares | See Refs. 39 and 40; may be worse than the standard Kalman filter. |
| 4. Covariance matrix in ruv coordinates | See Refs. 37 and 32; also Sec. V and Refs. 15 and 25. |
| 5. Add gradient of Kalman filter gain with respect to unknown parameter to algorithm | See Ref. 35. |
| 6. Preferred order of scalar measurement processing | See Ref. 24 and Sec. IV. |
| 7. Virtual decoupling of covariance matrix | See Ref. 36. |
| 8. Quasi-decoupling of covariance | See Sec. VI. |

## VI. FALSE OBSERVABILITY

A phenomenon that has not been widely noted in the literature, but which is common to most of the applications in Table I, is called "false cross-range observability." Briefly, this effect is due to an overoptimism on the part of the (linearized) Kalman filter with respect to its ability to derive cross-range estimates from accurate measurements in the range direction. The effect is particularly bothersome early in track, when the inevitable noisiness of the cross-range position estimates gives the illusion of a changing measurement direction and an associated triangulation effect. In a fully coupled filter, this false observability is present in both cross-range directions. If the covariance matrix is completely decoupled, as in an RPCC filter, this effect is removed; however, the filter is no longer capable of taking advantage of the true cross-range observability (in the range-velocity plane) provided by the line of sight rotation. The partially decoupled RVCC/CR filter benefits from the true observability, while eliminating the false observability in the out-of-plane direction; the benefits are obtained, however, only if the velocity direction is well known so that the RVCC system can be properly oriented, and this is generally not true early in track.

The identification of this problem is due to K. Brown of IBM. The effect is particularly acute in radars such as in Table I, owing to the large ratio of angle to range measurement error (both expressed in rectilinear coordinates). Thus, the basic cause of this phenomenon is the same as ill-conditioning, but it is demonstrably a distinct nonlinear effect. It turns out, however, that a special type of decoupling mitigates this effect also. The details of decoupling the covariance matrix to avoid false cross-range observability without suffering a significant loss in the benefit of covariance coupling were developed by Daum and Brown. A key ingredient in this algorithm is the so-called Joseph form of the error covariance update equations, for reasons that have nothing to do with ill-conditioning. In particular, the Kalman filter gain matrix is computed using a totally decoupled covariance matrix early in track; however, the error covariance matrix itself is propagated using the partially coupled form with Joseph's form of the update

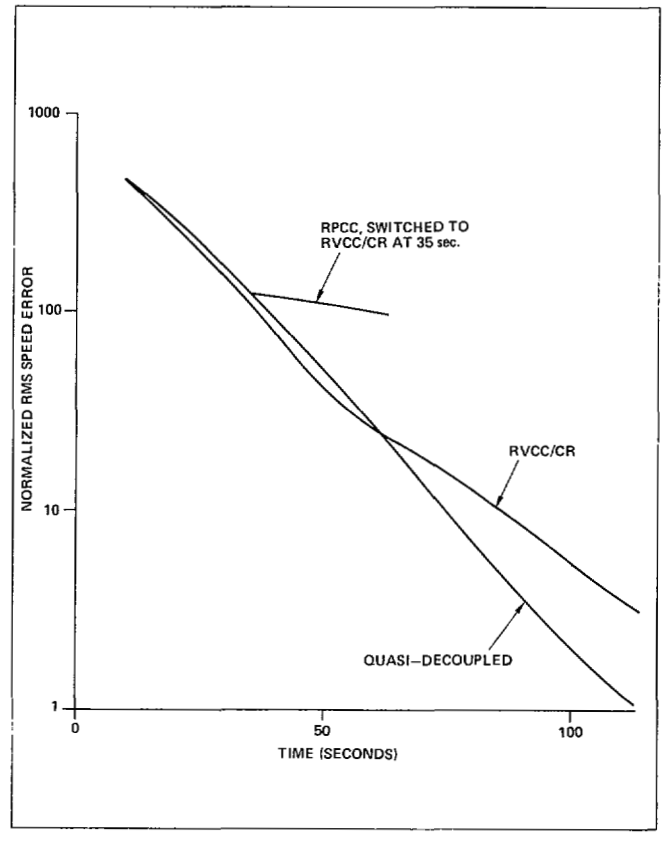


Fig. 8. Use of quasi-decoupling to overcome effects of false observability.

equation. This is the etymology of the term "quasi-decoupled"; in one sense, the filter is totally decoupled, but in another sense, it is not. The Joseph form of the update equation is used here because it correctly propagates the error covariance matrix (except for nonlinear effects) for any Kalman filter gain matrix, whether or not the gain is optimal. In the present case, the decoupled filter in early track ignores the degradation of range estimation which results from the poor angle rate estimates via the centrifugal ($r\dot{\theta}^2$) component of $\ddot{r}$. It is this degradation which is kept track of by the Joseph algorithm in order to avoid overoptimism in range. It is essential that the algorithm be told that the early gains are suboptimal due to the decoupling, and that the Joseph form be used to maintain a realistic covariance matrix; otherwise, performance can deteriorate markedly.

Quasi-decoupling improves performance by deferring the time at which covariance coupling affects the Kalman filter gain. At this time, the cross-range rate estimates deduced from radar angular measurements alone are sufficiently accurate to suppress false observability. Intuitively, quasi-decoupling makes the Kalman filter less greedy. In some sense, this method is an ad hoc approximation to Ljung's algorithm (Method 5). Fig. 8 presents results from a Monte Carlo comparison (25 runs) of three six-state RVCC tracking filters, and shows the improvement in speed estimation when quasi-decoupling is employed. Also presented is the performance achieved when the filter is simply changed from RPCC to RVCC/CR (at 35 s), without utilizing the Joseph form for covariance propagation.

## VII. Summary

The use of covariance coordinates of various kinds for decoupling of Kalman trackers yields the threefold advantage of reduced computational cost, alleviation of ill-conditioning, and mitigation of nonlinear effects. In comparison to covariance-matrix factorization techniques (item 3 of Table II), these decoupling approaches are attractive because of their computational efficiency. They are particularly appropriate for tracking problems because their success depends on statistical symmetries, and these are generally readily predictable in such problems. The relative appropriateness of the various decoupling approaches in any particular application depends on the directionality properties of the measurement errors and dynamic errors. Significant line-of-sight rotation rates may require modifications to the algorithms, including partial coupling and covariance-matrix rotation operations.

## References


[1] E. Brookner, *Radar Technology*. Dedham, MA: Artech, 1977.
[2] K. J. Stein, "Cobra Judy phased array radar tested," *Aviat. Week Space Technol.*, vol. 115, pp. 70–73, Aug. 1981.
[3] E. Filer and J. Hartt, "Cobra Dane wideband pulse compression system," presented at IEEE EASCON, Washington, DC, Sept. 1976.
[4] G. W. Johnson, "Choice of coordinates and computational difficulty," *IEEE Trans. Automat. Contr.*, vol, AC-19, pp. 77–78, Feb. 1974.
[5] R. E. Kalman, "Toward a theory of difficulty of computation in optimal control," in *Proc. IBM Scientific Comput. Symp. on Contr. Theory and Appl.*, 1966.
[6] G. J. Bierman and C. L. Thornton, "Numerical comparison of Kalman filter algorithms," *Automatica*, vol. 13, pp. 23–35, 1977.
[7] K. R. Brown, A. O. Cohen, E. F. Harrold, and G. W. Johnson, "Covariance coordinates—A key to efficient radar tracking," presented at IEEE EASCON, 1977.
[8] E. F. Beckenbach and R. Bellman, *Inequalities*. Berlin, Germany: Springer-Verlag, 2nd rev. printing, 1965.
[9] G. J. Bierman, *Factorization Methods for Discrete Sequential Estimation*. New York: Academic, 1977.
[10] J. H. Wilkinson, *Rounding Errors in Algebraic Processes*. Englewood Cliffs, NJ: Prentice-Hall, 1963.
[11] A. N. Tikhonov and V. Y. Arsenin, *Solutions of Ill-Posed Problems*. Washington, DC: Winston, 1977.
[12] D. M. Young and R. T. Gregory, *A Survey of Numerical Mathematics, Vol. II*. Reading, MA: Addison-Wesley, 1973.
[13] F. H. Schlee, C. J. Standish, and N. F. Toda, "Divergence in the Kalman filter," *AIAA J.*, vol. 5, pp. 1114–1120, June 1967.
[14] S. F. Schmidt, J. D. Weinberg, and J. S. Lukesh, "Application of Kalman filtering to the C-5 guidance and control system," ch. 13 in *Theory and Applications of Kalman Filtering*, C. T. Leondes, Ed. AGARD 139, 1970, pp. 312–313.
[15] G. W. Johnson, "Controllability, observability, and computational difficulty," in *24th Annu. South-West IEEE Conf. Rec.*, 1972.
[16] R. B. Blackman, "Methods of orbit refinement," *Bell Syst. Tech. J.*, vol. 43, May 1964.
[17] R. H. Battin, "A statistical optimizing navigation procedure for space flight," *ARS J.*, vol. 32, pp. 1681–1696, Nov. 1962.
[18] B. M. Irons, "Roundoff criteria in direct stiffness solutions," *AIAA J.*, vol. 6, pp. 1308–1312, 1968.
[19] W. C. Rheinbolt, "On measures of ill-conditioning for nonlinear equations," *Math. Comput.*, vol. 30, pp. 104–111, Jan. 1976.
[20] H. W. Sorenson, "On the error behavior in linear minimum variance estimation problems," *IEEE Trans. Automat. Contr.*, vol. AC-12, pp. 557–562, Oct. 1967.
[21] N. Morrison, *Introduction to Sequential Smoothing and Prediction*. New York: McGraw-Hill, 1969.
[22] P. G. Kaminski, A. E. Bryson, and S. F. Schmidt, "Discrete square root filtering: A survey of current techniques," *IEEE Trans. Automat. Contr.*, vol. AC-16, pp. 727–735, Dec. 1971.
[23] R. A. Monzingo and T. W. Miller, *Introduction to Adaptive Arrays*. New York: Wiley, 1980.
[24] D. M. Leskiw and K. S. Miller, "Nonlinear estimation with radar observations," *IEEE Trans. Aerosp. Electron. Syst.*, vol. AES-18, pp. 192–200, Mar. 1982.
[25] R. J. Fitzgerald, "On reentry vehicle tracking in various coordinate systems," *IEEE Trans. Automat. Contr.*, vol. AC-19, pp. 581–582, Oct. 1974.
[26] M. Athans, R. H. Whiting, and M. Gruber, "A suboptimal estimation algorithm with probabilistic editing for false measurements with applications to target tracking with wake phenomena," *IEEE Trans. Automat. Contr.*, vol. AC-22, pp. 372–384, June 1977.
[27] R. A. Singer, R. G. Sea, and K. Housewright, "Derivation and evaluation of improved tracking filters for use in dense multitarget environments," *IEEE Trans. Inform. Theory*, vol. IT-20, pp. 423–432, July 1974.
[28] Y. Bar-Shalom, "Tracking methods in a multitarget environment," *IEEE Trans. Automat. Contr.*, vol. AC-23, pp. 618–626, Aug. 1978.
[29] R. J. Fitzgerald, "Simple tracking filters: Steady-state filtering and smoothing performance," *IEEE Trans. Aerosp. Electron. Syst.*, vol. AES-16, pp. 860–864, Nov. 1980. See also corrections, vol. AES-17, p. 305, Mar. 1981.
[30] K. R. Brown, A. O. Cohen, E. F. Harrold, and G. W. Johnson, "Safeguard track filter design, Part I," IBM Fed. Syst. Div., IBM Rep. 75-0103-M19, Dec. 1976.
[31] M. Wold, G. Kelly, B. Birkholz, and L. Cady, "ARTS-III augmented tracking study," Fed. Aviation Admin. Rep. FAA-RD-73-27, AD-758 886, June 1972.
[32] R. K. Mehra, "A comparison of several nonlinear filters for reentry vehicle tracking," *IEEE Trans. Automat. Contr.*, vol. AC-16, pp. 307–319, Aug. 1971.
[33] R. J. Fitzgerald, "Effects of range-Doppler coupling on chirp radar tracking accuracy," *IEEE Trans. Aerosp. Electron. Syst.*, vol. AES-10, pp. 528–532, July 1974.
[34] P. E. Mantey, "Eigenvalue sensitivity and state-variable selection," *IEEE Trans. Automat. Contr.*, vol. AC-13, pp. 263–269, June 1968.
[35] L. Ljung, "Asymptotic behavior of the extended Kalman filter as a parameter estimator for linear systems," *IEEE Trans. Automat. Contr.*, vol. AC-24, pp. 36–50, Feb. 1979.
[36] K. Brown, D. Bedford, and D. Sweeney, "The virtually coupled sufficient statistics filter," IBM Int. Rep., Jan. 18, 1980.

[37] R. P. Wishner, R. E. Larson, and M. Athans, "Status of radar tracking algorithms," presented at the Symp. on Nonlinear Estimation Theory and Appl., 1970.
[38] R. Henriksen, "The truncated second-order nonlinear filter revisited," *IEEE Trans. Automat. Contr.*, vol. AC-27, pp. 247–251, Feb. 1982.
[39] B. T. Fang, "A nonlinear counterexample for batch and extended sequential estimation algorithms," *IEEE Trans. Automat. Contr.*, vol. AC-21, pp. 138–139, Feb. 1976.
[40] B. E. Schutz, J. D. McMillan, and B. D. Tapley, "Comparison of statistical orbit determination methods," *AIAA J.*, Nov. 1974.
[41] R. J. Fitzgerald, "Divergence of the Kalman filter," *IEEE Trans. Automat. Contr.*, vol. AC-16, pp. 736–747, Dec. 1971.
[42] —, "Graphical transformations of 2×2 covariance matrices," *IEEE Trans. Automat. Contr.*, vol. AC-13, pp. 751–753, Dec. 1968.
[43] M. L. Andrade Netto, L. Gimeno, and M. J. Mendes, "On the optimal and suboptimal nonlinear filtering problem for discrete-time systems," *IEEE Trans. Automat. Contr.*, vol. AC-23, pp. 1062–1067, Dec. 1978.
[44] P. J. Courtois, *Decomposability*. New York: Academic, 1977.
[45] R. E. Kalman, "New methods in Wiener filtering theory," in *Proc. Symp. Eng. Appl. of Random Function Theory and Probability*, F. Kozin and J. L. Bogdanoff, Eds. New York: Wiley, 1963.

**Frederick E. Daum** was born in Orange, NJ, on March 20, 1947. He received the B.S. degree in electrical engineering from the Newark College of Engineering, Newark, NJ, in 1969, and the M.S. degree in decision and control theory from Harvard University, Cambridge, MA, in 1972.

From 1972 to 1974 he did research on nonlinear continuous-time estimation theory at Harvard University. He is currently a Principal Engineer at Raytheon Company, Wayland, MA, on the staff of the Advanced System Engineering Department. He has developed, analyzed, and tested numerous algorithms for both exoatmospheric and endoatmospheric radar applications, including Cobra Dane, PAVE PAWS, Cobra Judy, and Sentry, as well as air traffic control and shipboard fire control systems. These algorithms include Kalman filters, track initiation, object classification, satellite versus missile discrimination, and radar pulse scheduling. In addition, he has analyzed radar system performance considering the effects of multiple target interference, jamming, ducting, Aurora, tropospheric refraction, ionospheric perturbations, target wake, and rocket exhaust plume. His present areas of interest are nonlinear discrete-time estimation theory and the use of adaptive Kalman filters for pattern recognition.

Mr. Daum is a member of Tau Beta Pi and Eta Kappa Nu.

**Robert J. Fitzgerald** was born in Hamilton, Ont., Canada. He received the B.A.Sc. degree from the University of Toronto, Toronto, Ont., Canada, in 1956, and the S.M., Mech. E., and Ph.D. degrees from the Massachusetts Institute of Technology, Cambridge, in 1957, 1958, and 1964, respectively. He also studied at the Ecole Nationale Supérieure de l'Aéronautique, Paris, France.

Since 1964 he has been employed in various divisions of the Raytheon Company, Bedford, MA, where his principal activities have been concerned with the application of estimation and control theory to radar tracking, inertial navigation, and missile intercept problems.

# Utilization of Modified Polar Coordinates for Bearings-Only Tracking

VINCENT J. AIDALA, MEMBER, IEEE, AND SHERRY E. HAMMEL, MEMBER, IEEE

*Abstract* — **Previous studies have shown that the Cartesian coordinate extended Kalman filter exhibits unstable behavior characteristics when utilized for bearings-only target motion analysis (TMA). In contrast, formulating the TMA estimation problem in modified polar (MP) coordinates leads to an extended Kalman filter which is both stable and asymptotically unbiased. Exact state equations for the MP filter are derived without imposing *any* restrictions on own-ship motion; thus, prediction accuracy inherent in the traditional Cartesian formulation is completely preserved. In addition, these equations reveal that MP coordinates are well-suited for bearings-only TMA because they automatically decouple observable and unobservable components of the estimated state vector. Such decoupling is shown to prevent covariance matrix ill-conditioning, which is the primary cause of filter instability. Further investigation also confirms that the MP state estimates are asymptotically unbiased. Realistic simulation data are presented to support these findings and to compare algorithm performance with respect to the Cramer–Rao lower bound (ideal) as well as the Cartesian and pseudolinear filters.**

Manuscript received March 12, 1982; revised August 27, 1982. This work was supported by the Naval Sea Systems Command under Code 63-R, Program Element 62633N, Project F33341/SF33323602, and the Naval Material Command under Code 08T1, Program Element 61152N, Project ZR00001/ZR0000101.

The authors are with the U.S. Naval Underwater Systems Center, Newport, RI 02840.